Journal of Physical Science, Vol. 35(3), 49–64, 2024

Preparation and Characterisations of Acrylic Epoxy/Polyethylene Glycol/Graphene Oxide Nanocomposites for Antibacterial Coating Applications

Wipsar Sunu Brams Dwandaru*, Duwi Susanto, Arina Fauza Achshuniya, Evan Fajri Mulia Harahap, Fika Fauzi and Suparno

Physics Education Department, Faculty of Mathematics and Natural Sciences, Universitas Negeri Yogyakarta, Jl. Colombo No. 1, Karangmalang, Sleman, Yogyakarta 55281, Indonesia

*Corresponding author: wipsarian@uny.ac.id

Published online: 30 November 2024

To cite this article: Dwandaru, W. S. B. et al. (2024). Preparation and characterisations of acrylic epoxy/polyethylene glycol/graphene oxide nanocomposites for antibacterial coating applications. *J. Phys. Sci.*, 35(3), 49–64. https://doi.org/10.21315/jps2024.35.3.4

To link to this article: https://doi.org/10.21315/jps2024.35.3.4

ABSTRACT: *This study addresses the urgent need for antibacterial coatings amid escalating concerns about pathogen contamination on various surfaces, particularly in healthcare settings and public spaces where infection control is critical. The development of durable and effective antibacterial coatings could significantly reduce harmful bacteria transmission and improve overall hygiene standards. Graphene oxide (GO) had exceptional antibacterial properties against a wide spectrum of bacteria. Here, the researchers explored the composite of GO with acrylic epoxy (AE) through the use of polyethylene glycol (PEG) to become AE/PEG/GO tertiary nanocomposites in enhancing GO's antibacterial efficacy. The objectives of this study were to prepare and characterise AE/PEG/GO nanocomposites and then investigate their antibacterial abilities against escherichia coli (E. coli) and staphylococcus aureus (S. aureus) bacteria. The GO was prepared using the modified Hummers method, which was mechanically stirred with AE and PEG to produce the AE/PEG/GO nanocomposites. This was followed by characterisations of the nanocomposites via ultraviolet-visible (UV-Vis) spectrophotometer, X-ray diffraction (XRD), Fourier transform infrared (FTIR) spectrometer and scanning electron microscope (SEM). The nanocomposites were then tested against E. coli and S. aureus bacteria by measuring the diameter of the inhibition zone (DIZ). The results showed that the absorption peak of GO was obtained at a wavelength of 236 nm. The diffraction pattern of the AE/PEG/GO nanocomposites showed amorphous structure with a small and wide peak at 2θ around 23°. The IR spectrum of the AE/PEG/GO nanocomposites indicated the presence of –OH, –CH_3, –CH_2, C=O, C–H, C–O and C=C functional groups.*

The surface morphology showed well-distributed nanocomposite coating onto glass slides with some micro islands. The nanocomposites exhibited promising antibacterial performance revealing higher efficacy against S. aureus compared to E. coli. This was shown by the performance of AE/PEG/GO coating in inhibiting S. aureus bacteria with 1.55 mm larger DIZ compared to the positive control. However, the AE/PEG/GO coating exhibited smaller DIZ than the positive control with a difference of 3.68 mm in inhibiting E. coli bacteria. This study unveiled a simple and straightforward approach in producing nanocomposites for antibacterial coatings shedding light on their potential applications in safeguarding surfaces against bacterial contamination.

Keywords: Graphene oxide (GO), AE/PEG/GO nanocomposites, antibacterial coating, escherichia coli, staphylococcus aureus

1. INTRODUCTION

Nanocomposites are one of the forefronts of materials having excellent physical and chemical properties for various and specific applications. A plethora of nanocomposites has been produced in many multidisciplinary fields to fulfill the needs of humans in their daily activities. One such application is in the antibacterial coating industry where one of the challenges is supplying superior coating materials having antibacterial properties, e.g., coatings for various surfaces. A coating material that is used extensively for various surfaces is acrylic epoxy (AE) spray paint. Recently, a heat resistant spray paint is used in the experimental set up of graphene-coated aluminum substrates to measure surface temperature.[1] However, surfaces may be contaminated by pathogenic bacteria that may be dangerous for human health.[2] Hence, one way to improve the property of spray paint is to inject antibacterial property into it. This may be fulfilled by adding antibacterial material, i.e., graphene oxide (GO) as an additive in the AE spray paint. Moreover, in order to strengthen the bonds between the spray paint and GO, polyethylene glycol (PEG) is used in the composites.

GO is a derivative of graphene. GO has many excellent properties, which make it one of the most applied nanomaterials in the world.[3] One of these is its exceptional antibacterial property, i.e., GO can be applied as antibacterial agent.[4] Many studies have been dedicated to explore the application and mechanisms of GO as antibacterial agent since more than a decade ago. Recently, the antibacterial property of reduced-GO (rGO) prepared via microbes was investigated against *escherichia coli* (*E. coli*).[5] As expected, cell membranes and oxidative stresses contribute to the antibacterial mechanism of the rGO. Previous results also show the marvel of GO in inhibiting various bacteria. The performance of GO nanosheets as bactericidal agent against various Gram-positive and Gram-negative bacteria, i.e., *E. coli*, *klebsiella pneumoniae* (*K. pneumoniae*), *pseudomonas*

aeruginosa (*P. aeruginosa*), *proteus mirabilis* (*P. mirabilis*), *serratia marcescens* (*S. marcescens*) and *staphylococcus aureus* (*S. aureus*) produces diameter inhibition zones (DIZs) of 39 mm, 41 mm, 38 mm, 27 mm, 39 mm and 38 mm, respectively.[6] This shows that GO is equally effective in inhibiting Gram-positive and Gram-negative bacteria.[4] The possible mechanisms for the ability of GO in killing the aforementioned bacteria hence producing clear zones surrounding the GO media are; (1) GO penetration through the outer layer of the bacteria disabling many important functions of the bacteria and (2) entrapment of the bacteria by the GO sheets such that the bacteria undergo mal-nutrition because they are cut off from the environment. On the other hand, several studies indicate that Gram-positive bacteria, e.g., *S. aureus*, are more susceptible to GO penetration and/or entrapment.[7,8] For Gram-negative bacteria, e.g., *E. coli*, the antibacterial activity of GO is resisted by the presence of an outer membrane layer of the bacteria.[9] Moreover, increasing the oxygen content of GO increases its ability as an antibacterial agent.[7]

As mentioned in the beginning, the performance of the GO as an antibacterial agent can be greatly improved by functionalising GO as nanocomposites, e.g., adding biocompatible polymer such as PEG. The addition of PEG prevents the immune system from phagocytising GO in the body.[10] Moreover, PEG may also be used as a binder to enhance the adhesive property of the nanocomposites, hence making it appropriate for coating material.[11] In this case, PEG is used as a binder for AE spray paint and the GO. Other nanocomposites have been produced with GO as one of the nano-scale components especially tailored to their antibacterial activity, e.g., silver nanoparticles (AgNP)/GO. As Ag is widely known to be an excellent antibacterial agent; it is naturally advantageous to combine it with GO in order to improve the composite's antibacterial ability.[12,13] In fact, high stability and activity of tertiary composites involving GO/PEG and AgNP have been produced to tackle the problem of GO/AgNP being prone to aggregation and sedimentation.[14] Other GO composites are used for antibacterial purposes, e.g., zinc oxide (ZnO)/GO, polypyrrole (PPy)/GO triboelectric nanogenerator electrode, and poly(3-hydroxybutyrate-co-3-hydoxypentanoate) (PHBV)/GO fibrous polymer membrane.[15–19] Hence, to the knowledge of the authors, the preparation of tertiary nanomaterial involving GO, PEG and AE for coating purposes enhanced with antibacterial property has not been conducted before.

The AE/PEG/GO tertiary nanocomposites can be viewed from two perspectives. First, the nanocomposites can be thought of as empowering the AE spray paint with the antibacterial ability of PEG/GO. On the other hand, the aforementioned nanocomposites can be viewed as a PEG/GO antibacterial material with a

coating ability of AE. In relation to the antibacterial property of GO and PEG, it is also worth mentioning the toxicity of these materials towards human and other organisms. According to recent research, GO may affect red blood cells and organs, such as skin, kidney and liver, which may be caused by oxidative stress, inflammation, genotoxicity and cytoxicity.[20] Furthermore, the toxicity of GO is dependent upon particle size, dosage, exposure time and functionalised compounds, hence making it possible for implementing GO materials under safe conditions by exploiting these factors.[21] On the other hand, PEG is a hydrophilic and biocompatible polymer, which is extensively used as diagnostic and therapeutic agents and surface coatings known as PEGylation, hence safe to be applied and FDA approved.[22] In fact, the addition of PEG in the PEG/GO nanocomposites enhances the safety of the nanocomposites. Hence, the objectives of the present study are to prepare and characterise the AE/PEG/GO nanocomposites. Moreover, the antibacterial ability of the nanocomposites coated on glass slides is tested against Gram-negative and Gram-positive bacteria, i.e., *E. coli* and *S. aureus*, respectively. In this study, the GO is prepared via the modified Hummers method. The characterisations of the AE/PEG/GO nanocomposites are conducted using ultraviolet-visible (UV-Vis) spectrophotometer, X-ray diffraction (XRD), Fourier transforms infrared (FTIR) spectroscopy and scanning electron microscope (SEM). The nanocomposites produced are coated onto clay ceramic and glass slide surfaces. The antibacterial property of the nanocomposites coated on the glass slides is then investigated via diameter of inhibition zones (DIZs) calculation.

2. METHODOLOGY

The materials used in this study included pure graphite powder (from Crocoweld Indonesia), sulfuric acid (H_2SO_4), sodium nitrate ($NaNO_3$), potassium permanganate ($KMnO_4$), distilled water, hydrogen peroxide (H_2O_2), hydrochloric acid (HCl), PEG and AE. All chemicals, except for graphite powder were obtained from Merck Indonesia. These materials were of analytical grades except for PEG and AE, which were technical grades.

The preparation of the GO was conducted as follows. GO powder was synthesised using a modified Hummers method. Initially, 30 mL of H_2SO_4 was stirred in a 500 mL beaker glass. Subsequently, 0.5 g of $NaNO_3$ and 1 g of pure graphite were slowly added to the solution, followed by stirring for 1 h. The beaker glass was then transferred to an ice bath to maintain a temperature between 10°C–20°C. Next, 3 g of $KMnO_4$ was gradually added to the solution, and stirring continued for 20 h. Following this, the beaker glass was removed from the ice bath and heated to reach a temperature of 40°C. Then, 150 mL of distilled water was added, and

stirring continued for 1 h at the same temperature. Subsequently, 5 mL of H_2O_2 was added to the solution and stirred for 1 h. This was followed by the addition of 10 mL of HCl, and stirring continued for an additional hour. The subsequent step involved washing with distilled water using a centrifuge until reaching a neutral pH. The solution was finally dried in an oven for 40 min at a temperature of 100°C to obtain the GO powder.

The AE/PEG/GO nanocomposites were prepared using the following steps. An amount of 3.3 g of GO was added to 10 mL of PEG and stirred for 10 min at room temperature. The solution was then sonicated using an ultrasonic cleaner for 10 min to break up any clumps of GO powder that might have formed. Next, 5 mL of AE was added to the solution and stirred for another 10 min. From this process, the AE/PEG/GO nanocomposites were obtained with a concentration of 0.22 g/mL. The AE/PEG/GO nanocomposites were now ready for use in the sample coating process. The coating process was conducted via the dip coating method. The materials being coated were clay ceramics and glass slides.

The optical properties of the samples were observed using the UV-Vis spectrophotometer Shimadzu UV-2450. The crystal structure was examined using XRD Rigaku Miniflex 600 Benchtop instrument. The functional groups of the samples were determined using FTIR Thermo Scientific Nicolet iS10. Finally, the surface morphology of the samples were investigated using an SEM JSM-6510LA instrument.

To prepare the bacterial cultures of *S. aureus* and *E. coli*, nutrient agar or Mueller-Hinton agar (MHA) was prepared in petri dishes. Subsequently, pure cultures of *S. aureus* and *E. coli* were taken and transferred to the agar media. Afterwards, the bacterial cultures were evenly spread on the surface of the agar. The Petri dishes were left to incubate at the appropriate temperature for 24 h allowing bacterial growth on the agar. Once this process was completed, the petri dishes with bacterial cultures were ready to be used in the antibacterial tests.

The next step involved testing the antibacterial property of the coated AE/PEG/GO nanocomposites against the *S. aureus* and *E. coli* bacterial cultures. Glass slides coated with the AE/PEG/GO nanocomposites were placed near the bacterial cultures on the agar surface. Subsequently, the petri dishes were incubated again at room temperature during the bacterial growth period. During the incubation, the diameter of the inhibition zone (DIZ) around the glass slides were observed and measured. The DIZs indicated the extent to which the nanocomposites were able to inhibit bacterial growth. The larger the DIZs, the stronger the antibacterial effect of the coated nanocomposites against *S. aureus* and *E. coli* bacteria.

3. RESULTS AND DISCUSSON

AE/PEG/GO nanocomposites are synthesised from GO, PEG and AE that are mixed together. The first material synthesised is GO. It is prepared from pure graphite powder via modified Hummer's method. The GO material fabricated in this study can be observed in Figure 1(a). It may be observed that the GO material obtained is in the form of dark bulky sheets. The GO sheets are then grounded into powder form so that it can be dispersed into AE/PEG/GO solutions. The AE/PEG/GO solution can be seen in Figure 1(b). The solution looks almost clear without any sediment and has brownish color. Finally, the coating of the AE/PEG/GO nanocomposites on clay ceramics and glass slides can be observed in Figure 1(c) and Figure 1(d), respectively. The coating layer cannot be observed with the naked eye, which shows excellent transparent coating. If the coated area observed meticulously under white light, one can barely see it shine.

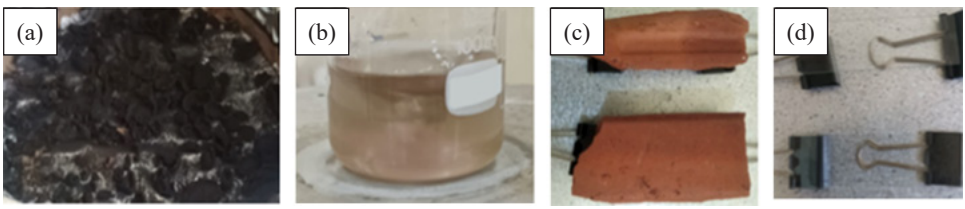

Figure 1: (a) The synthesised GO in the form of dark bulky sheets, (b) AE/PEG/GO nanocomposites in the form of brownish solution, (c) AE/PEG/GO coating onto clay ceramic and (d) surfaces.

Figure 2 shows the absorption spectral of various samples obtained in this study. The GO has a characteristic high absorption peak at 236 nm (see Figure 2 – purple line). The absorption peak of the GO is in line with the finding from another literature that has an absorption peak of GO at 235.5 nm, which refers to the electronic transitions of $\pi \rightarrow \pi^*$ that also shows the existence of C=C functional groups in the synthesised GO.[23] This is of course different from the absorption spectrum of graphite (Figure 2 – black line), which shows the absorption spectrum of graphite powder.[24] The AE sample (Figure 2 – blue line) shows two absorption peaks at 204 nm and 256 nm, whereas the PEG sample (Figure 2 – red line) only shows a shouldering peak at 224 nm. Finally, the AE/PEG/GO nanocomposites (Figure 2 – green line) show several shouldering peaks, which are a combination of absorption peaks of the nanocomposites' individual components. The shouldering peaks of 204 nm, 224 nm and 236 nm are observed in the absorption spectrum of the nanocomposites, which indicate the presence of AE, PEG and GO in the nanocomposites, respectively.

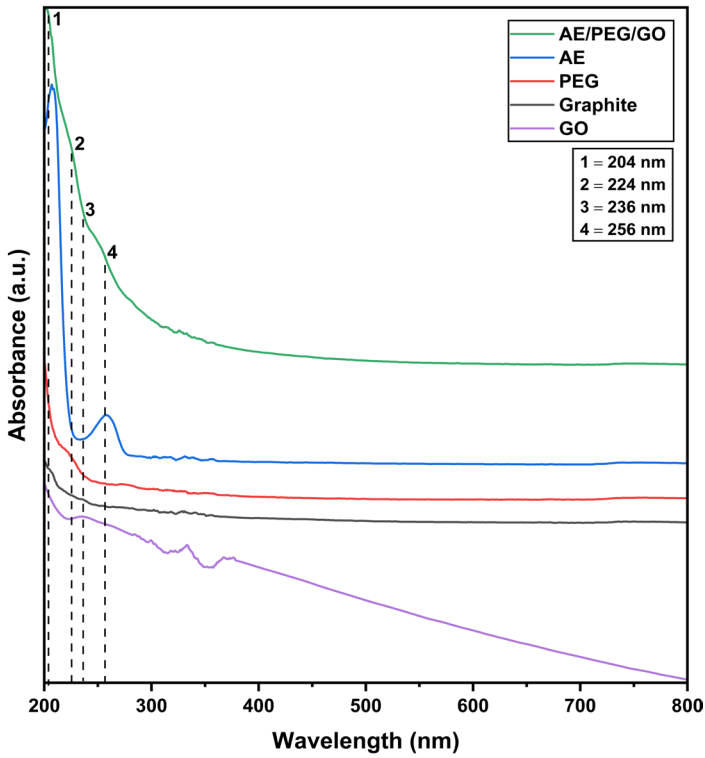

Figure 2: Absorption spectra of the samples; GO (purple line), graphite (black line), PEG (red line), AE (blue line) and AE/PEG/GO nanocomposites (green line).

The XRD spectra of the samples can be seen in Figure 3, which show the crystallinity of the samples. Figure 3(b) shows the diffraction pattern of GO, which has low intensity peaks at 10.12° and 44.16° due to diffraction plane indices of (001) and (002), respectively. The absence of high intensity peak of graphite at 26° (see Figure 3[a]) indicates that the graphite powder is successfully exfoliated and form graphene multilayer with abundant of oxygen. On the other hand, Figure 3(c) shows the diffraction pattern of AE/PEG/GO nanocomposites that are coated on the glass slides. A relatively low peak of GO appears at 9.7°. This indicates small amount of GO mixed with the AE and PEG, so that the GO peak is just barely seen. Moreover, a dominant broad peak indicates AE and PEG peaks. AE has high intensity peaks at 20.1° and 22.3°, meanwhile the PEG has high intensity peaks at 19° and 23°. The AE and PEG are deformed in the process of synthesising the nanocomposites, which makes the micro strain becomes wider and not uniform, and hence causing the broadening of the peak.[25]

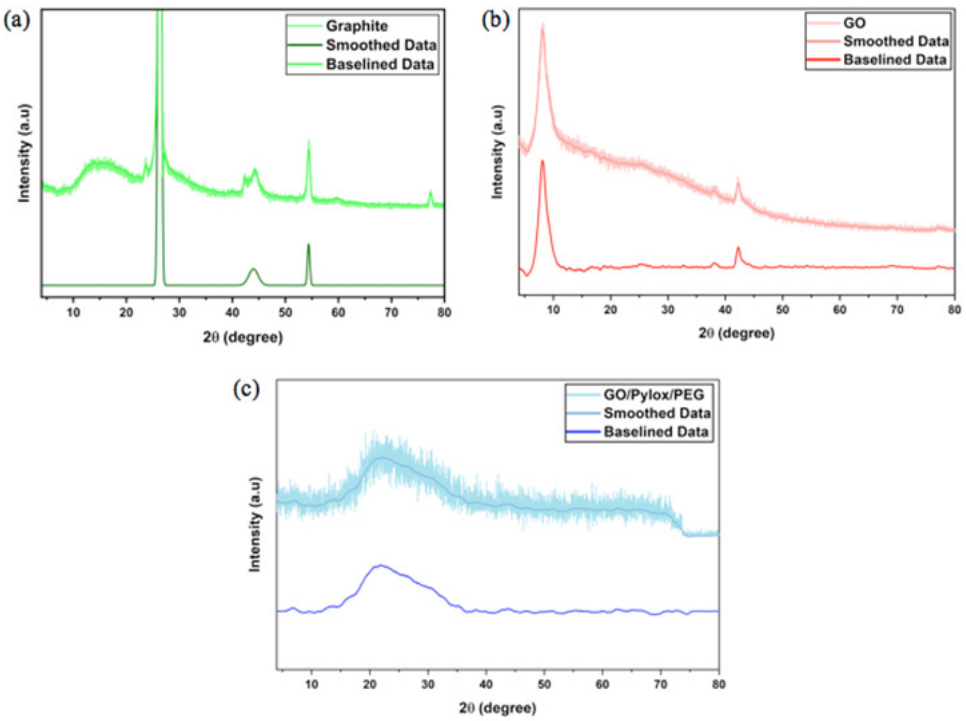

Figure 3: (a) Diffraction patterns of graphite, (b) GO and (c) AE/PEG/GO nanocomposites.

The functional groups contained in the synthesised samples are shown in Figure 4. The FTIR spectrum of the GO is shown in Figure 4(a) – green line. There are several distinctive bands in the transmission spectrum. A broad and intense band at 3,400 cm^{-1} indicates O–H group of stretching vibrations that makes GO hydrophilic.[26] Additionally, two highly recognisable bands at 1,720 cm^{-1} and 1,620 cm^{-1} are situated in the center of the spectrum and can be associated with the stretching modes of C=O and C=C bonds, respectively. One broad band between 1,377 cm^{-1} and 1,407 cm^{-1} is assigned to the O–H bending. Furthermore, a broad band between 1,075 cm^{-1} and 1,095 cm^{-1} and a sharp band at 802 cm^{-1} can be found in the fingerprint region of the spectrum. These bands likely correspond to C–O stretching and C=C bending, respectively. The FTIR spectrum of AE (Figure 4[a] – blue line) shows a small broad band at 3,548 cm^{-1}–3,448 cm^{-1} due to intermolecular O–H stretching bonding. The strong band at 2,930 cm^{-1} corresponds to the C–H stretching of terminal methyl groups (CH_3) in the triglyceride chains, while the methylene moieties (CH_2) exhibit a stretching band at 2,869 cm^{-1}. Additionally, a strong sharp band at 1,724 cm^{-1} indicates C=O stretching from α,β-unsaturated ester, while the methyl group exhibits a bending C–H band at 1,453 cm^{-1}. A band at 1,158 cm^{-1} exhibits

sharp and strong transmission peak that indicates C–O stretching ester groups. Furthermore, in the fingerprint region of the spectrum, a medium sharp band at 758 cm^{-1} and a strong sharp peak at 700 cm^{-1} can be observed. These bands likely correspond to C–H and C=C bending, respectively.

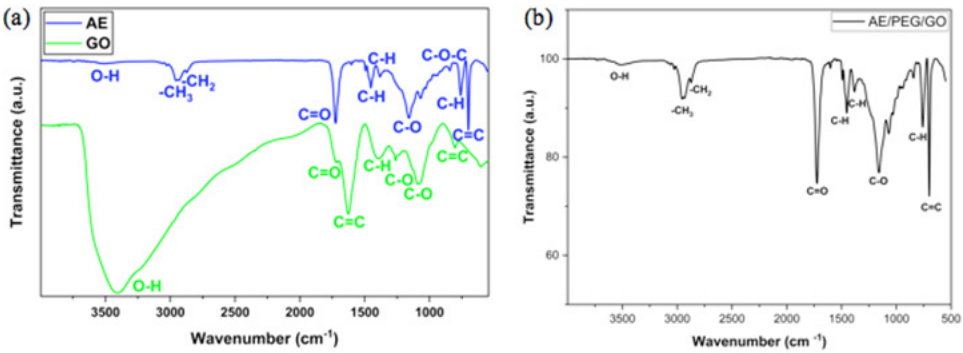

Figure 4: (a) FTIR spectra of GO (green line) and AE (blue line) and (b) AE/PEG/GO nanocomposites.

The FTIR spectrum of AE/PEG/GO nanocomposites is depicted in Figure 4(b). The functional groups present in the AE/PE/GO nanocomposites appear to be a combination of the functional groups of GO and AE. This suggests the high purity of the nanocomposites. The transmission bands of PEG closely resemble those of AE, indicating similarity in their functional groups. The presence of GO is evident from the broad bands observed between 3,500 cm^{-1} and 3,300 cm^{-1} corresponding to the O–H functional groups of GO. Additionally, the functional groups of AE reappear, including $–CH_3$, $–CH_2$, C=O, C–H, C–O and C=C with nearly identical wavenumbers.

The surface morphologies of GO and coated AE/PEG/GO nanocomposites can be observed from the SEM results as shown in Figure 5. It can be seen from Figure 5(a) that GO has sheet-like surfaces and stacked on top of each other. Clearly, it can be concluded that the graphene layers have been exfoliated. The SEM result of the GO strengthened the characterisation results of the GO from UV-Vis, XRD and FTIR that were discussed before. This sheet-like form can make it easier for the GO material to form nanocomposites with other materials since it has a large surface area and is hydrophilic. Figure 5(b) shows the surface morphology of AE/PEG/GO nanocomposites coated onto glass slides (see Figure 1[d]). The coating looks well distributed on top of the glass slide with some micro islands. The coating looks identical, so it can be concluded that GO is well combined with AE and PEG to form mono dispersed nanocomposites coating. This makes the antibacterial properties work effectively on the whole

surface area.[27] The SEM results further corroborate the FTIR findings, indicating that the functional groups of GO are highly minimal to the extent of being nearly imperceptible due to the successful integration of GO into the AE/PEG/GO nanocomposites.

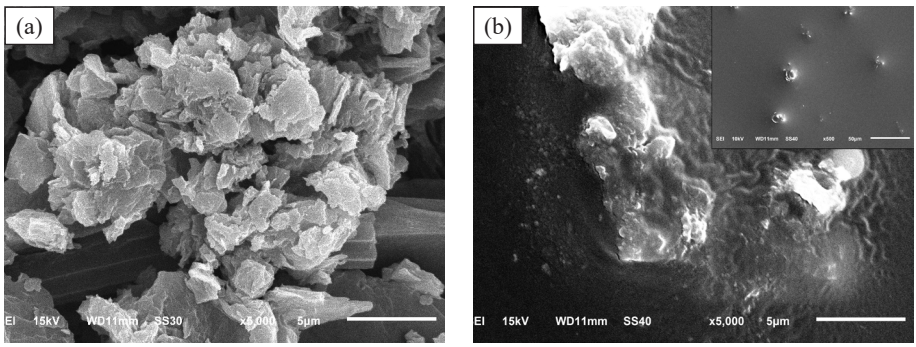

Figure 5: (a) Surface morphology images of GO and (b) AE/PEG/GO nanocomposites coated onto glass slides.

Figure 6 illustrates the disc diffusion method utilised to investigate the antibacterial performance of the AE/PEG/GO nanocomposites' coating on glass slides against the Gram-positive *S. aureus* and Gram-negative *E. coli* bacteria, alongside the conventional chloramphenicol as a positive antibacterial control. The use of GO in the AE/PEG/GO coating is examined for its influence on antibacterial effectiveness. GO, known for its antimicrobial properties, can disrupt bacterial cell membranes, impede enzyme activity and induce oxidative stress, ultimately leading to bacterial demise.[4,28]

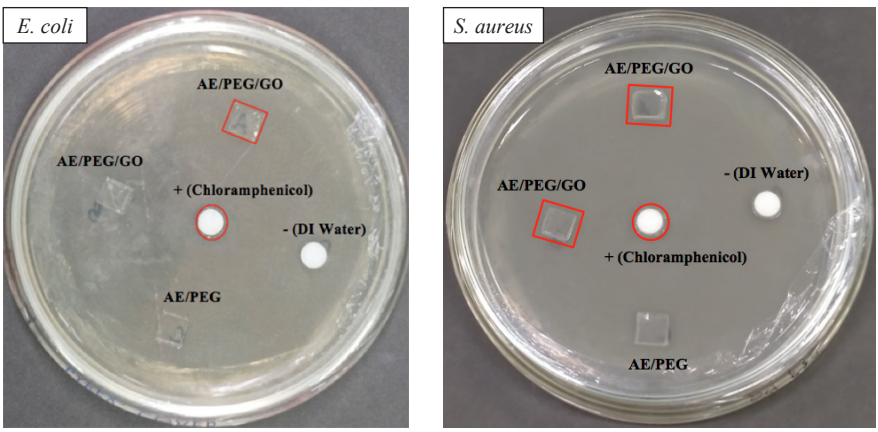

Figure 6: The disc diffusion method used to measure the DIZ of the samples against *E. coli* and *S. aureus* bacteria. The circle and rectangle in red represent the DIZ of the samples.

The antibacterial performance results of the coated AE/PEG/GO nanocomposites are depicted in Figure 7, showcasing the measurement of the formed DIZs. These zones denote areas around the antimicrobial substance where bacterial growth is impeded. The DIZ serves as an indicator of the antimicrobial agent's efficacy. Discrepancies in the DIZs between the nanocomposite coatings and chloramphenicol may stem from differing modes of action. *S. aureus* bacteria possess a thick peptidoglycan layer in their cell walls making them difficult to be penetrated and/or destroyed by antibacterial agents. However, *S. aureus* may still be vulnerable to certain antibacterial agents and/or antibiotics that can target and disrupt the peptidoglycan layer more effectively.[29] On the other hand, *E. coli* bacteria have an additional outer membrane composed of lipopolysaccharides (LPS), acting as a barrier that can hinder the penetration and efficacy of some antibacterial agents, resulting in reduced susceptibility compared to Gram-positive bacteria.[30]

The antibacterial performance evaluation reveals that the AE/PEG and the AE/PEG/GO coatings differ by 0.55 mm and 0.66 mm in terms of the DIZs against *S. aureus* and *E. coli* bacteria, respectively, signifying a significant impact of the GO material added to the coating material. When comparing the DIZs of the AE/PEG/GO coating with the positive control (see Figure 7[a]), the AE/PEG/GO coating exhibits a wider DIZ against the Gram-positive *S. aureus* bacteria, with a difference of 1.55 mm, indicating its enhanced efficacy in inhibiting *S. aureus*. Conversely, the AE/PEG/GO coating demonstrates a smaller DIZ against the Gram-negative *E. coli* bacteria, with a difference of 3.68 mm (see Figure 7[b]), signifying a greater effectiveness of the positive control in inhibiting *E. coli*.

The larger inhibition zones observed in the coating with GO is due to its efficacy in disrupting cell membranes and inducing stress on Gram-positive bacterial walls.[31] The positive control operates by directly interfering with protein synthesis through cell membrane disruption. The diverse modes of action and specific targets of the antibacterial agents may account for their differential effectiveness against various bacterial species, potentially explaining the excellent performance of the AE/PEG/GO coating against *S. aureus* compared to *E. coli*. The smaller inhibition zone of the AE/PEG/GO coating against *E. coli* might result from difficulties in penetrating complex bacterial walls of Gram-negative bacteria, specifically *E. coli*.

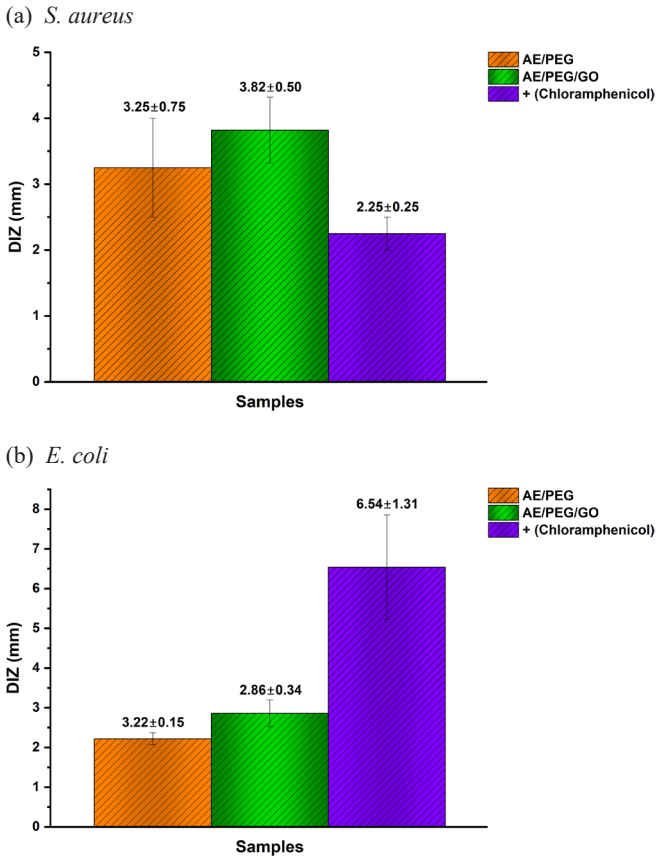

Figure 7: The DIZs of AE/PEG, AE/PEG/GO nanocomposites and chloramphenicol againts *S. aureus* and *E. coli* using the disc diffusion method.

The functionality of antibacterial coating of AE/PEG/GO nanocomposites involves immobilising or trapping the GO within the coating matrix. This immobilisation restricts the movement of GO, thereby potentially enhancing its efficacy against bacteria.[32] By keeping the GO in close proximity to the surface, it effectively targets and disrupts bacterial cell membranes or vital functions, either inhibiting their growth or leading to their demise. In contrast, liquid-based positive control may disperse and move away from the surface, resulting in less focused and potentially less effective action against bacteria over time. Coatings of AE/PEG/GO nanocomposites with the trapped GO offer a more controlled and sustained release, hence maintaining their antibacterial potency for longer durations.[31] However, due to the trapped nature of GO as an antibacterial agent, the resulting inhibition zones may not be as extensive as that of antibacterial agents that can disperse into the surrounding environment.

4. CONCLUSION

The preparation and characterisations of AE/PEG/GO nanocomposites followed by their coating onto clay ceramic and glass slide surfaces proved successful and displayed a transparent coating. The synthesised GO exhibited an absorption peak at 236 nm and pronounced XRD intensity peaks at 10.12° and 44.16°. Notably, the AE/PEG/GO coating displayed characteristic broad peaks between 18.41° and 33.76°. The FTIR spectrum confirmed the presence of AE, GO and AE/PEG/GO nanocomposite materials. The surface morphology images revealed sheet-like surface characteristics in the GO structure indicative of successful layer-by-layer graphite exfoliation. Moreover, the surface morphology of the AE/PEG/GO nanocomposites coated on the glass slide displayed a well-distributed pattern with micro islands resulting from controlled heating during the coating process demonstrating the successful integration of GO, AE and PEG to form uniformly dispersed nanocomposite coating. The antibacterial tests conducted using the disc diffusion method revealed enhanced antibacterial performance of the nanocomposites upon the addition of GO. The performance of AE/PEG/GO coating proved more effective in inhibiting *S. aureus* bacteria with 1.55 mm larger DIZ compared to the positive control. However, towards *E. coli* bacteria, the AE/PEG/GO coating exhibited smaller DIZ than the positive control with a difference of 3.68 mm. As for future research, further characterisations should be conducted for the GO using atomic force microscope (AFM) and/or Raman spectroscopy. Moreover, in order to determine the optimum concentration of the AE/PEG/GO nanocomposites in inhibiting bacteria, antimicrobial perfomance tests of the AE/PEG/GO nanocomposite coatings with varying concentations are also recommended for further studies. Additionally, exploring alternative evaluation methods for antibacterial properties, such as broth microdilution, CFU killing assays, and time-kill studies, would provide a more thorough assessment of the nanocomposites' effectiveness.

5. ACKNOWLEDGEMENTS

The authors' deepest gratitude is given to the Mathematics and Natural Sciences Faculty, Universitas Negeri Yogyakarta for funding this study through the Research Group Scheme 2023 with contract number: B/136/UN34.13/PT.01/03/2023.

6. REFERENCES

1. Goh, J. Y. H., Hung, Y. M. & Tan, M. K. (2020). Extraordinarily enhanced evaporation of water droplets on graphene-nanostructured coated surfaces. *Int. J. Heat Mass Transf.*, 163, 120396. https://doi.org/10.1016/j.ijheatmasstransfer.2020.120396
2. Kisla, D. et al. (2023). Recent developments in antimicrobial surface coatings: Various deposition techniques with nanosized particles, their application and environmental concerns. *Trends Food Sci. Tech.*, 135, 144–172. https://doi.org/10.1016/j.tifs.2023.03.019
3. Saputra, A. M. A. et al. (2022). Synthesis and characterization of graphene oxide/chitosan composite membranes from natural waste. *J. Phys. Sci.*, 33(3), 63–79. https://doi.org/10.21315/jps2022.33.3.5
4. Ng, I. M. J. & Shamsi, S. (2022). Graphene oxide (GO): A promising nanomaterial against infectious diseases caused by multidrug-resistant bacteria. *Int. J. Mol. Sci.*, 23(16), 9096. https://doi.org/10.3390/ijms23169096
5. Zhou, Y. et al. (2023). Antibacterial activity of reduced graphene oxide prepared by microbe. *Mater. Today Sustain.*, 22, 100341. https://doi.org/10.1016/j.mtsust.2023.100341
6. Aunkor, M. T. H. et al. (2020). Antibacterial activity of graphene oxide nanosheet against multidrug resistant superbugs isolated from infected patients. *R. Soc. Open Sci.*, 7(7), 200640. https://doi.org/10.1098/rsos.200640
7. Bousiakou, L. G. et al. (2022). Synthesis and characterization of graphene oxide (GO) sheets for pathogen inhibition: *Escherichia coli*, *Staphylococcus aureus* and *Pseudomonas aeruginosa*. *J. King Saud Univ. Sci.*, 34, 102002. https://doi.org/10.1016/j.jksus.2022.102002
8. Ghanim, R. R., Mohammad, M. R. & Hussien, A. M. A. (2018). Antibacterial activity and morphological characterization of synthesis graphene oxide nanosheets by simplified Hummer's method. *Biosci. Biotechnol. Res. Asia*, 15(3). https://www.biotech-asia.org/?p=30850
9. Akhavan, O. & Ghaderi, E. (2010). Toxicity of graphene and graphene oxide nanowalls against bacteria. *ACS Nano*, 4(10), 5731–5736. https://doi.org/10.1021/nn1011390x
10. Jihad, M. A. et al. (2021). Polyethylene glycol functionalized graphene oxide nanoparticles loaded with *Nigella sativa* extract: A smart antibacterial therapeutic drug delivery system. *Molecules*, 26(11), 3067. https://doi.org/10.3390/molecules26113067
11. Zhang, D. et al. (2018). Preparation of expanded graphite/polyethylene glycol composite phase change material for thermoregulation of asphalt binder. *Constr. Build. Mater.*, 169, 513–521. https://doi.org/10.1016/j.conbuildmat.2018.02.167
12. Cobos, M. et al. (2020). Graphene oxide-silver nanoparticle nanohybrids: Synthesis, characterization, and antimicrobial properties. *Nanomater.*, 10(2), 376. https://doi.org/10.3390/nano10020376
13. Naseem, T. & Waseem, M. (2022). A comprehensive review on the role of some important nanocomposites for antimicrobial and wastewater applications. *Int. J. Environ. Sci. Technol.*, 19, 2221–2246. https://doi.org/10.1007/s13762-021-03256-8

14. Bao, Y. et al. (2023). Polyethylene glycol modified graphene oxide-silver nanoparticles nanocomposite as a novel antibacterial material with high stability and activity. *Colloids Surf. B: Biointerfaces*, 229, 113435. https://doi.org/10.1016/j.colsurfb.2023.113435
15. Ma, W. et al. (2022). Synthesis and characterization of ZnO-GO composites with their piezoelectric catalytic and antibacterial properties. *J. Environ. Chem. Eng.*, 10(3), 107840. https://doi.org/10.1016/j.jece.2022.107840
16. Dharmalingam, P. et al. (2019). Mechanism of inhibition of graphene oxide/zinc oxide nanocomposite against wound infection causing pathogens. *Appl. Nanosci.*, 10(2), 827–849. https://10.1007/s13204-019-01152-9
17. Wang, Y. -W. et al. (2014). Superior antibacterial activity of zinc oxide/graphene oxide composites originating from high zinc concentration localized around bacteria, *ACS Appl. Mater. Interfaces*, 6(4), 2791–2798. https://doi.org/10.1021/am4053317
18. Jannesari, M. et al. (2023). Boosting on-demand antibacterial activity using electrical stimulations from polypyrrole-graphene oxide triboelectric nanogenerator. *Nano Energy*, 112, 108463. https://doi.org/10.1016/j.nanoen.2023.108463
19. Ou, Y. R. et al. (2023). Preparation of antibacterial PHBV/GO nanocomposite membranes via electrospinning. *Mater. Today Commun.*, 35, 106370. https://doi.org/10.1016/j.mtcomm.2023.106370
20. Sepahi, M. M. & Azizi, M. (2024). Graphene oxide nanotoxicity: A comprehensive analysis. In E. W., Wambu (Eds.). *Chemistry of Graphene – Synthesis, Reactivity, Applications and Toxicities*. London: IntechOpen, 87. https://doi.org/10.5772/intechopen.111179
21. Ghulam, A. N. et al. (2022). Graphene oxide (GO) materials – Applications and toxicity on living organisms and environment. *J. Func. Biomater.*, 13, 77. https://doi.org/10.3390/jfb13020077
22. Yao, X. et al. (2023). Poly(ethylene glycol) alternatives in biomedial applications. *Nano Today*, 48, 101738. https://doi.org/10.1016/j.nantod.2022.101738
23. Fauzi, F. et al. (2022). Synthesis of polyacrylamide/graphene oxide/clove essential oil composite via physical adsorption method for potential antibacterial packaging applications. *Nano-Struct. Nano-Objects*, 32, 100908. https://doi.org/10.1016/j.nanoso.2022.100908
24. Pimpang, P., Wongrerkdee, S. & Choopun, S. (2019). Charge transfer improvement of ZnO-based dye-sensitized solar cells modified with graphite nanosheets and bilayer photoelectrode structures. *Ferroelectrics*, 552, 1–9. https://doi.org/10.1080/00150193.2019.1653077
25. Janković, B. et al. (2023). Biomineral nanocomposite scaffold ($CaCO_3$/PVA based) carrier for improved stability of vitamin D3: Characterization analysis and material properties. *J. Mater. Sci.*, 58(15), 6580–6601. https://doi.org/10.1007/s10853-023-08453-z
26. Cheng, M. –M. et al. (2019). Synthesis of graphene oxide/polyacrylamide composite membranes for organic dyes/water separation in water purification. *J. Mater. Sci.*, 54(1), 252–264. https://doi.org/10.1007/s10853-018-2828-9

27. Sarraf, S. H., Rastegari, S. & Soltanieh, M. (2023). Deposition of mono dispersed Co–CeO_2 nanocomposite coatings by a sol-enhanced pulsed reverse electroplating: Process parameters screening. *J. Mater. Res. Technol.*, 23, 3772–3789. https://doi.org/10.1016/ j.jmrt.2023.02.036
28. Bhatt, S. et al. (2023). Recent advances and mechanism of antimicrobial efficacy of graphene-based materials: A review. *J. Mater. Sci.*, 58, 7839–7867. https://doi .org/10.1007/s10853-023-08534-z
29. Esposito, S. et al. (2023). New antibiotics for *Staphylococcus aureus* infection: An update from the World Association of Infectious Diseases and Immunological Disorders (WAidid) and the Italian society and anti-infective therapy (SITA). *Antibiotics*, 12(4), 742. https://doi.org/10.3390/antibiotics12040742
30. Emiola, A. et al. (2016). Crosstalk between the lipopolysaccharide and phospholipid pathways during outer membrane biogenesis in *Escherichia coli*. *Proc. Natl. Acad. Sci. USA*, 113(11), 3108–3113. https://doi.org/10.1073/pnas .1521168113
31. Shamsi, S. et al. (2022). Stability, toxicity, and antibacterial potential of gallic acid-loaded graphene oxide (GAGO) against methicillin-resistant *Staphylococcus aureus* (MRSA) strains. *Int. J. Nanomedicine*, 17, 5781–5807. https://doi.org/ 10.2147/ijn.s369373
32. Wang, Y. et al. (2020). Enhancing the thermo-stability and anti-bacterium activity of lysozyme by immobilization on chitosan nanoparticles. *Int. J. Mol. Sci.*, 21(5), 1635. https://doi.org/10.3390/ijms21051635